

The effect of driving temperature ratio  $(T_r - T_w)/T_w$  on streamwise spacing  $\lambda$  measured on wax cones is shown in Figs. 4 and 5 for constant values of  $M_e$  and  $p_e$ . The streamwise spacing increases nearly linearly with the temperature ratio. A similar observation is presented in Fig. 1 of Ref. 3, where plexiglas which is also a liquifying ablation material was used. Reference 3 shows clearly that the pattern wavelength was nearly doubled when the stagnation temperature was increased from  $T_{st} = 750^\circ\text{K}$  to  $1070^\circ\text{K}$ . It may be possible that the driving temperature dependence of the pattern size is characteristic of liquifying ablation materials. Camphor test results are not yet available.

#### 4.3 Pattern Motion

For a few tests with wax models (both axisymmetric and two-dimensional) a movie was taken during the complete testing period. It showed a slow "creeping" motion of the whole crosshatched pattern in the streamwise direction of the order of 1 wavelength/10 sec.

#### References

- <sup>1</sup> Williams, E. P., "Experimental Studies of Ablation Surface Patterns and Resulting Roll Torques," AIAA Paper 69-180, New York, 1969.
- <sup>2</sup> Laganelli, A. L. and Nestler, D. E., "Surface Ablation Patterns: A phenomenology Study," AIAA Paper 68-671, Los Angeles, 1968.
- <sup>3</sup> Canning, T. N. et al., "Orderly Three-dimensional Processes in Turbulent Boundary Layers on Ablating Bodies," AGARD Supplement to Conference Proceedings No. 30, May 1968.
- <sup>4</sup> Mirels, H., "Origin of Striations on Ablative Materials," *AIAA Journal*, Vol. 7, No. 9, Sept. 1969, pp. 1813-1814.
- <sup>5</sup> Tobak, M., "Hypothesis for the Origin of Cross-Hatching," *AIAA Journal*, Vol. 8, No. 2, Feb. 1970, pp. 330-334.
- <sup>6</sup> Probst, P. F. and Gold, H., "Cross-Hatching: A Material Response Phenomena," *AIAA Journal*, Vol. 8, No. 2, Feb. 1970, pp. 364-366.
- <sup>7</sup> Charwat, A. F., "Exploratory Studies on the Sublimation of Slender Camphor and Naphtalene Models in a Supersonic Wind Tunnel," RM-5506-ARPA, July 1968, Rand Corporation.

## Computation of Chebycheff Optimal Control

GERALD J. MICHAEL\*

United Aircraft Research Laboratories,  
East Hartford, Conn.

### I. Introduction

THE majority of optimal control problems appearing in the literature consist essentially of a system defined by the vector differential equation

$$\dot{x} = f(x, u, t), \quad x(t_0) = x_0, \quad u \in U \quad (1)$$

and a Bolza-type optimality criterion

$$J[u] = \int_{t_0}^{t_f} h(x, u, t) dt + F[x(t_f), t_f]$$

where  $x$  represents the vector state of the system,  $U$  denotes a set of admissible controllers, and  $t_0, t_f$  denote initial and final times, respectively. Optimal control  $u^*$  is defined as that control in  $U$  which minimizes the performance criterion

Received November 9, 1970; revision received January 25, 1971. The author gratefully acknowledges valuable discussions with and the programming assistance of G. J. Thrasher of the Turbo Power and Marine Division of United Aircraft Corporation.

\* Research Engineer, Simulation Laboratory.

$J$ , i.e.,  $u^*$  is defined by  $J[u^*] = \min_u J[u]$ . Well-known analytic and computational techniques exist for the solution of such Bolza-type optimization problems. On the other hand, there are many situations when the performance criterion  $J$  is not conveniently representable as a line integral. Such situations occur when it is desired to minimize the maximum or peak value of some pertinent time function as, for instance, power or percent overshoot. In these cases the performance criterion is given by  $J[u] = \max_t g[x(t)]$  and optimal control  $u^*$  is defined by  $J[u^*] = \min_u \max_t g[x(t)]$  for  $u \in U$  and  $t \in [t_0, t_f]$ . Performance criteria of this type are not generally amenable to a Bolza formulation and are, in fact, termed Chebycheff performance criteria after the Russian mathematician Chebycheff whose basic investigations in the 19th century led to the formulation and the solution of a broad class of min-max problems. For the Chebycheff optimal control problem, however, very few results are available.

Neustadt<sup>1</sup> considered a Chebycheff-type problem in which it is desired to transfer a linear system from one given state to another while minimizing the control effort, where effort is defined as the maximum control amplitude. Johnson<sup>2</sup> provided valuable insight into the Chebycheff problem by deriving certain geometric properties of a Chebycheff optimal controller, but his technique for explicitly determining optimal control is not amenable to digital computation and except for relatively simple systems, is prohibitively difficult to implement.

In this paper a general method is demonstrated for the efficient computation of Chebycheff optimal control for nonlinear systems. The algorithm is used to determine a Chebycheff optimal controller for the minimum flight path angle climb to station of an airbreathing vehicle whose thrust and fuel flow rate are characterized by a thrust coefficient and a specific impulse both of which are given as tabular functions of Mach number. Advantages of the proposed algorithm are pointed out as well as potential pitfalls which may be encountered in its implementation. The purpose of this paper is to demonstrate, by its application to a relatively sophisticated nonlinear system typical of those which occur in many practical aerospace flight control problems, that the proposed algorithm is a computationally feasible means of solving Chebycheff optimal control problems as well as to point out certain of its limitations.

### II. Chebycheff Algorithm

The dynamic system is represented by Eq. (1) with  $t_0$  specified, a final time  $t_f \geq t_0$  implicitly defined by  $\Omega[x(t_f)] = 0$ , and  $x_0 \in X$  where  $X$  is interpreted as the set of all states controllable by some  $u \in U$  to the manifold defined by  $\Omega(x) = 0$ . It is assumed that  $X$  is nonempty. The variational problem considered here is the minimization of

$$J[u] = \max_t g[x(t)] \quad (2)$$

with respect to  $u \in U$  for  $t \in [t_0, t_f]$  and subject to the differential constraint (1). In order to develop a computational procedure for approximating the Chebycheff optimal controller  $u^*$ , a theorem<sup>3</sup> is invoked which states that if  $h(t)$  is non-negative, single-valued, bounded, and continuous function on  $[t_0, t_f]$  then

$$\max_t h(t) = \lim_{q \rightarrow \infty} \left\{ \int_{t_0}^{t_f} [h(t)]^q dt \right\}^{1/q}$$

Then if  $g$  satisfies the previous conditions the Chebycheff criterion (2) can be replaced by the infinite sequence of performance criteria

$$J_q[u] = \left\{ \int_{t_0}^{t_f} [g(x(t))]^q dt \right\}^{1/q}, \quad q = 1, 2, \dots$$

Since minimization of  $J$  is equivalent to minimization of the

Table 1 Numerical convergence

$q$	2	4	6	8	10	12	14	16	18	20	22
$\ \Delta\theta_q^*\ $	...	0.7735	0.5252	0.3745	0.2887	0.2238	0.1588	0.1457	0.1406	0.1428	0.1398
$\ \Delta J_q^*\ $	...	1.328	0.3205	0.1364	0.0705	0.0459	0.0206	0.0100	0.0037	0.0010	0.0037

Bolza criterion

$$J_q[u] = \int_{t_0}^{t_f} \{g[x(t)]\}^q dt \quad (3)$$

then  $u_q^*$  can be obtained for each  $q$  by minimizing  $J_q$  and the Chebycheff optimal controller  $u^*$  can be approximated by  $u_q^*$  for large  $q$ . Control  $u_q^*$  is used to initiate the search for  $u_{q+1}^*$ . Hence, the Chebycheff problem is replaced by an infinite sequence of Bolza problems the solutions of which converge to the Chebycheff solution. In practice, it may be necessary to normalize the integrand of Eq. (3). This situation is discussed in Sec. IV.

The computational technique presented here for the solution of Chebycheff optimal control problems was briefly mentioned in Ref. 2 and is conspicuously characterized by its simplicity and ease of implementation. But yet, as illustrated in the next section, the algorithm is capable of solving a formidable nonlinear Chebycheff optimization problem arising in the flight control of an airbreathing vehicle.

### III. Chebycheff Optimal Flight Control of an Airbreathing Vehicle

In this section, the Chebycheff algorithm is implemented to determine the minimum flight path angle climb to station of an airbreathing vehicle whose thrust and fuel flow rate are characterized by a thrust coefficient  $C_T(M)$  and a specific impulse  $I_{sp}(M)$  both of which are given as tabular functions of Mach number. Vehicle dynamics are given by

$$\begin{aligned} \dot{x} &= \frac{R}{R+h} v \cos \gamma, \quad \dot{h} = v \sin \gamma \\ \dot{v} &= -g_0 \left( \frac{R}{R+h} \right)^2 \sin \gamma + S_c C_T(M) \frac{\rho(h)v^2}{2m} \cos(\theta - \gamma) - \\ &\quad \frac{\rho(h)v^2}{2m} [C_{D_{min}}(M) + C_{D_{L\alpha}}(\theta - \gamma)^2] S_{ref} \\ \dot{\gamma} &= \frac{V \cos \gamma}{R+h} - \frac{g_0}{V} \left( \frac{R}{R+h} \right)^2 \cos \gamma + \\ &\quad C_{N\alpha}(\theta - \gamma) \frac{\rho(h)v}{2m} S_{ref} + S_c C_T(M) \frac{\rho(h)v}{2m} \sin(\theta - \gamma) \\ \dot{m} &= - \left[ S_c C_T(M) \frac{\rho(h)v^2}{2} \right] / g_0 I_{sp}(M) \end{aligned} \quad (4)$$

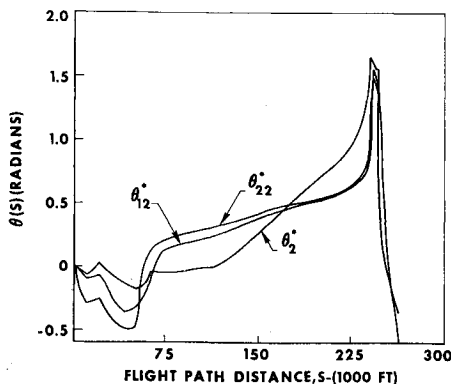


Fig. 1 Vehicle attitude  $\theta^*$ .

where  $x, h, v, \gamma$ , and  $m$  are the range (ft), altitude (ft), velocity (fps), flight path angle (rad), and mass (slugs) of the vehicle, respectively. Vehicle attitude  $\theta$  represents the single control variable. Constants and parameters appearing in these equations are  $R = 20,926,607$  ft, Earth's radius in the equatorial plane;  $g_0 = 32.174$  ft/sec<sup>2</sup>, gravitational acceleration in the equatorial plane;  $S_c$  = engine capture area = 32.2 ft<sup>2</sup>;  $S_{ref}$  = wing reference area = 500 ft<sup>2</sup>;  $C_{DL}$  = aerodynamic coefficient associated with drag due to lift = 2.1 rad<sup>-2</sup>;  $C_N$  = lift curve slope = 2.1 rad<sup>-1</sup>;  $C_{D_{min}}(M)$  = aircraft profile drag coefficient as a function of Mach number;  $I_{sp}(M)$  = engine specific impulse as a function of Mach number, sec;  $C_T(M)$  = thrust coefficient as a function of Mach number;  $\rho(h)$  = atmospheric density as a function of altitude, slugs/ft<sup>3</sup>. The state vector at  $t = 0$  is specified as  $x(0) = 0$  ft,  $h(0) = 500$  ft,  $v(0) = 780$  fps,  $\gamma(0) = 0$  rad,  $m(0) = 1119$  slugs and the final time  $t_f$  is implicitly defined by  $h(t_f) = 70,000$  ft,  $v(t_f) = 2518$  fps,  $\gamma(t_f) = 0.27$  rad along with a specified final flight path distance of 260,000 ft. Air density  $\rho(h)$  and speed of sound are those given by the ICAO Standard Atmosphere of 1956. Curves characterizing  $C_T(M)$ ,  $I_{sp}(M)$ ,  $C_{D_{min}}(M)$  are identical to those presented on page 11 of Ref. 4. These curves and parameters are representative of the second stage of a typical rocket-boosted ramjet vehicle. Thrasher<sup>4,5</sup> used Bolza-type optimality criteria to obtain minimum time and minimum fuel controllers for this system.

The optimality criterion considered here is of the Chebycheff type and is given by  $J[\theta] = \max_t |\gamma(t)|$  so that the Chebycheff optimal controller  $\theta^*$  is defined as  $J[\theta^*] = \min_\theta \max_t |\gamma(t)|$ . Hence,  $\theta^*$  represents that control which takes the system (4) from a given initial state to a given terminal manifold and yields the minimum peak magnitude of flight path angle  $\gamma(t)$  for  $t \in [0, t_f]$ .

Optimal control  $\theta^*$  was approximated by first replacing the Chebycheff criterion  $J$  by the indexed Bolza criterion

$$J_q[\theta] = \int_0^{t_f} [\gamma^2(t)]^q dt.$$

A min- $H$  technique<sup>6</sup> was then used to compute  $\theta_q^*$ . The program was initiated by selecting a control  $\theta$  which satisfied the system end point constraints.  $\theta_q^*$  was then used to initiate the search for  $\theta_{q+2}^*$ . To improve computational accuracy the flight path distance  $s$  was taken as the independent variable via the transformation  $dt = (1/v)ds$ . Figures 1 and 2 illustrate  $\theta_2^*$ ,  $\theta_{12}^*$ , and  $\theta_{22}^*$  along with the corresponding optimum flight path angles  $\gamma_2^*$ ,  $\gamma_{12}^*$ ,  $\gamma_{22}^*$ .

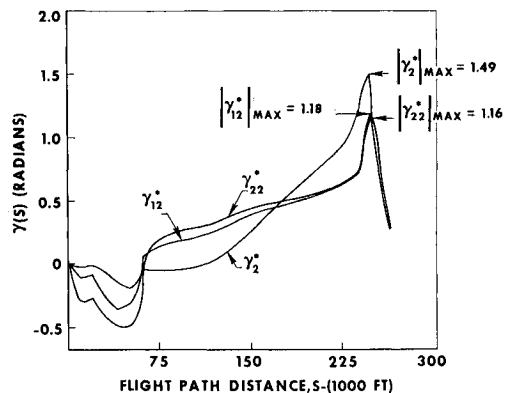


Fig. 2 Flight path angle  $\gamma^*$ .

The pertinent results are summarized in Table 1 where

$$\|\Delta\theta_q^*\| \triangleq \sum_i |\theta_q^*(s_i) - \theta_{q-1}^*(s_i)|$$

$$\|\Delta J_q^*\| \triangleq |(J_q^*)^{1/q} - (J_{q-1})^{1/q-1}|$$

and the  $s_i$  represent 126 equispaced points along the flight path. Univac 1108 computer run time to  $q = 12$  and  $q = 22$  was 4.43 and 9.27 minutes, respectively. It is interesting to note that after the first six passes the maximum flight path angle had been reduced from 1.49 rad ( $86^\circ$ ) to 1.18 rad ( $68^\circ$ ) but an additional five passes resulted in a further reduction of only 0.02 rad. Moreover, although there exists a significant difference between  $\theta_{12}^*(s)$  and  $\theta_{22}^*(s)$  for smaller  $s$ , as  $s$  approaches that point at which  $\max |\gamma(t)|$  occurs  $\theta_{12}^*$  and  $\theta_{22}^*$  become nearly identical. A similar statement can be made for  $\gamma_{12}^*$  and  $\gamma_{22}^*$ . This behavior is due to the fact that the Chebycheff optimality criterion concerns itself only with the maximum of a time function and ignores other values of that function. These results tend to substantiate an observation made by Johnson<sup>2</sup> concerning the non-uniqueness of Chebycheff optimal controllers.

#### IV. Comments and Conclusions

A principal advantage of the Chebycheff algorithm presented here stems from the fact that the Chebycheff solution is obtained by solving a sequence of standard Bolza problems for which well-known analytic and computational techniques are available. Thus, results obtained over the past decade concerning the relative merits of first- and second-order search techniques, state and control variable constraints, etc., can be utilized in the Chebycheff algorithm. On the other hand, certain inherent limitations must be considered. In particular, the curves presented in Fig. 2 and the possibility of a nonunique optimal controller point to the desirability of using a norm on performance as a stopping criterion rather than a norm on control. However, in some problems  $J_q^*$  may exceed computer numeric limits for large  $q$  before  $\|\Delta J_q^*\|$  has reached a stopping criterion. In these cases it becomes necessary to replace  $J_q$  as given in Eq. (3) by

$$J_q[u] = \int_{t_0}^{t_f} [g(t)/\hat{g}]^q dt$$

where  $\hat{g}$  is a normalizing constant used to maintain  $J_q$  within reasonable limits and to increase the rate of convergence of  $u_q^*$  to  $u^*$ .

For the optimization problem presented in the previous section, a search technique based only on first-order variations was used to compute  $u_q^*$  for each  $q$ . In general, it is to be expected by reasons of continuity that  $u_q^*$  would not be vastly dissimilar to  $u_{q+1}^*$ . Since  $u_q^*$  is used to initiate the search for  $u_{q+1}^*$  it thus appears that utilization of a second-order algorithm could achieve savings in total computer run time as well as increased accuracy.

#### References

- Neustadt, L. C., "Minimum Effort Control Systems," *Journal of Society for Industrial and Applied Mathematics*, Vol. 1, No. 1, 1962, pp. 16-31.
- Johnson, C. D., "Optimal Control with Chebyshev Minimax Performance Index," *Joint Automatic Control Conference*, AIAA, New York, 1966, pp. 345-358.
- Taylor, A. E., *Introduction to Functional Analysis*, Wiley, New York, 1958, p. 91.
- Thrasher, G. J., "Optimal Programming for Aircraft Trajectories Utilizing a New Strategy for Handling Inequality Constraints," AIAA Paper 69-812, Los Angeles, 1969.
- Thrasher, G. J., "Application of the Augmented Min-H Strategy to the Problem of Minimum-Time Atmospheric Trajectories," UARL Rept. G-110137-5, Oct. 1968, United Aircraft Research Laboratories, East Hartford, Conn.
- Gottlieb, R. G., "Rapid Convergence to Optimum Solutions using a Min-H Strategy," *AIAA Journal*, Vol. 5, No. 2, Feb. 1967, pp. 322-329.

## Influence of Film Thickness on the Calibration of Thin-Film-Gage Backing Materials

RONALD K. HANSON\*

Cranfield Institute of Technology, England

THIN-FILM resistance thermometers are now standard transducers in shock tubes and other high-speed-flow devices where a measurement of the transient surface temperature can be processed to yield, for example, heat-transfer rates,<sup>1,2</sup> thermal conductivities of gases,<sup>3,4</sup> and thermal accommodation coefficients.<sup>5,6</sup> In each of these experiments one needs to know the value of the property  $(\rho c \lambda)^{1/2}$  for the film backing material where  $\rho$ ,  $c$ , and  $\lambda$  are, respectively, the substrate density, specific heat and thermal conductivity. Experience has shown that this quantity should be determined dynamically over a time interval comparable with the test time of the temperature-measurement experiment, and a very convenient pulse-heating technique has been developed for this purpose.<sup>7</sup> It is generally assumed, in obtaining  $(\rho c \lambda)^{1/2}$  of the substrate with this method, that the heat conduction is one dimensional, the substrate behaves as a semi-infinite medium and the film thickness is negligible. For short times, however, this model breaks down owing to the finite heat capacity of the film, and this effect can be important if one wishes to calibrate the gage for short-duration experiments, or if the film thickness is great. (Of course the model also breaks down for large times when two- and three-dimensional effects come into play.) This Note presents a solution for the response of a finite-thickness gage during pulse heating and suggests a simple, approximate means of obtaining  $(\rho c \lambda)^{1/2}$  from pulse-heating data when finite-thickness effects are important.

Typically in the experiment a step voltage is applied to a simple bridge circuit, with the thin-film gage forming one arm of the bridge, thus subjecting the gage to a known (constant) heating pulse. The resulting bridge out-of-balance voltage, which can be monitored on an oscilloscope, is thus equivalent to the gage temperature-time history. The experiment is generally performed with the gage exposed to air and then repeated with the gage immersed in a standard liquid. If one neglects the film thickness and assumes that the heat is liberated at the surface of the backing material,  $(\rho c \lambda)^{1/2}$  for the backing material follows directly from a known value of  $(\rho c \lambda)^{1/2}$  for the liquid and the ratio of the bridge output voltages for the two experiments at the same time after pulse initiation.<sup>7</sup> In the present model we consider that heat is generated uniformly throughout an infinite film, of thickness  $\delta$ , mounted on a semi-infinite expanse of backing material. The film is bounded on the opposite side by a semi-infinite expanse of gas or liquid. Denoting the film as region 1, the solid substrate as region 2, and the gas or liquid as region 3, the appropriate equations to solve for one-dimensional heat conduction are (for constant thermal properties)

$$\partial^2 T_1 / \partial x^2 - (1/\alpha_1) \partial T_1 / \partial t = -A/\lambda_1 \quad (1)$$

and

$$\partial^2 T_{2,3} / \partial x^2 - (1/\alpha_{2,3}) \partial T_{2,3} / \partial t = 0 \quad (2)$$

where  $T$  is the temperature,  $\alpha$  is the thermal diffusivity ( $\alpha = \lambda/\rho c$ ), and  $A$  is the heat-generation rate per unit volume. Anticipating the usual experimental arrangement we take  $A$  constant. The heat generation is assumed to begin at  $t = 0$  and the film-substrate interface is taken at  $x = 0$ , with the

Received October 21, 1970.

\* Presently an NRC Postdoctoral Fellow at NASA Ames Research Center, Moffett Field, Calif.